nature communications

Article

https://doi.org/10.1038/s41467-024-45395-9

Interacting topological quantum chemistry in 2D with many-body real space invariants

Received: 27 May 2023

Accepted: 19 January 2024

Published online: 08 February 2024

Check for updates

Jonah Herzog-Arbeitman [1] ✉, B. Andrei Bernevig [1,2,3] & Zhi-Da Song [1,4]

The topological phases of non-interacting fermions have been classified by their symmetries, culminating in a modern electronic band theory where wavefunction topology can be obtained from momentum space. Recently, Real Space Invariants (RSIs) have provided a spatially local description of the global momentum space indices. The present work generalizes this real space classification to interacting 2D states. We construct many-body local RSIs as the quantum numbers of a set of symmetry operators on open boundaries, but which are independent of the choice of boundary. Using the $U(1)$ particle number, they yield many-body fragile topological indices, which we use to identify which single-particle fragile states are many-body topological or trivial at weak coupling. To this end, we construct an exactly solvable Hamiltonian with single-particle fragile topology that is adiabatically connected to a trivial state through strong coupling. We then define global many-body RSIs on periodic boundary conditions. They reduce to Chern numbers in the band theory limit, but also identify strongly correlated stable topological phases with no single-particle counterpart. Finally, we show that the many-body local RSIs appear as quantized coefficients of Wen-Zee terms in the topological quantum field theory describing the phase.

The symmetries of a Hamiltonian are essential to the classification of topological phases in crystals. For instance, the Ten-Fold Way[1,2], Topological Quantum Chemistry (TQC)[3,4], and symmetry indicators[5–8] have redefined our understanding of non-interacting electronic states of matter with the symmetry group of the Hamiltonian taking center stage. The success of this program motivates us to extend its reach to interacting Hamiltonians where many-body effects accompany band topology in the groundstate[9–38]. This work focuses on 2D systems with space group G and $U(1)$ charge conservation at an integer filling per unit cell.

The classifications of single-particle topology originally relied on momentum space calculations such as the Wilson loop[39–46] and band structure irreps[7,8,47–50]. Physically, however, nontrivial topology is completely diagnosed in real space where a topological index serves as an obstruction to the atomic limit, defined by a representation of the groundstate with localized, symmetric Wannier states[51–53]. Recently, ref. 54 extended this idea to symmetry-protected phases by developing Real Space Invariants (RSIs) – local indices which can be considered as Noether charges associated to discrete symmetries – which may be calculated from the irreps formed by the Wannier states in the unit cell, even in fragile phases[55,56]. These RSIs are gauge-invariant and classify all 2D and 3D symmetry eigenvalue-indicated single-particle topology[5,6,57–59], but may not detect some topological states which are classified by cohomology or not protected by symmetry[60–64]. Our paper extends this technique by defining many-body RSIs (henceforth referred to as RSIs for brevity) of two types.

First, we construct local RSIs on open boundary conditions (OBCs) in all 2D point groups. These RSIs classify adiabatically distinct many-body atomic states[9,45,65–68]. We then define many-body fragile topological states[6,9,41,69–72] by an obstruction to all many-body atomic limit states and derive their topological invariants in terms of inequalities between the RSIs and the $U(1)$ particle number. We also

[1]Department of Physics, Princeton University, Princeton, NJ 08544, USA. [2]Donostia International Physics Center, P. Manuel de Lardizabal 4, 20018 Donostia-San Sebastian, Spain. [3]IKERBASQUE, Basque Foundation for Science, Bilbao, Spain. [4]International Center for Quantum Materials, School of Physics, Peking University, Beijing 100871, China. ✉e-mail: jonahh@princeton.edu

present an exactly solvable model verifying that interactions trivialize certain fragile non-interacting states identified by our classification. To study many-body stable topological states[3,73–75], we introduce global RSIs defined on periodic boundary conditions and show that they are many-body stable topological invariants. Finally, we show that the local RSIs appear as quantized coefficients in the topological response theory generalizing the Chern-Simons action of a Chern insulator.

Our theory provides an elementary classification of symmetry-protected Chern and fragile topological phases, provides an explicit connection between many-body and single-particle topological indices substantiated by exactly solvable model Hamiltonians, and proposes a fundamental relation between these topological indices defined on the lattice and the topological quantum field theory that describes their universal behavior.

Results

Many-body local RSIs

Axiomatically, we define a many-body topological state by an obstruction to adiabatically deforming it into a many-body atomic (trivial) state while respecting the symmetries of the space group G. The results of this paper rely on the following definition. A many-body atomic state is any state which is adiabatically connected to a trivial many-body atomic limit which is **(1)** non-degenerate, **(2)** spatially decoupled, and **(3)** endowed with a many-body gap. This limit allows for arbitrarily strong interactions in the Hamiltonian as long as they are strictly local. A many-body atomic limit is the groundstate of the tight-binding Hamiltonian

$$H_{AL} = \sum_{\mathbf{R},\mathbf{r}} H_{\mathbf{R},\mathbf{r}}, \qquad H_{\mathbf{R},\mathbf{r}} = T_{\mathbf{R}} H_{\mathbf{r}} T_{\mathbf{R}}^{\dagger} \tag{1}$$

where $\mathbf{R}$ are the lattice vectors, $T_{\mathbf{R}} \in G$ are the translation operators, $\mathbf{r}$ are the locations of orbitals in the unit cell, and $H_{\mathbf{R},\mathbf{r}}$ is supported only on the orbitals at $\mathbf{R}+\mathbf{r}$ (there are no hoppings). This ensures $[H_{\mathbf{R},\mathbf{r}}, H_{\mathbf{R}',\mathbf{r}'}] = 0$ and thus the groundstate of H can be written as $|GS\rangle = \prod_{\mathbf{R},\mathbf{r}} \mathcal{O}_{\mathbf{R},\mathbf{r}}|0\rangle$ and $\mathcal{O}_{\mathbf{R},\mathbf{r}}$ creates the (possibly correlated) groundstate of $H_{\mathbf{R},\mathbf{r}}$. In the thermodynamic limit, the filling is $\nu = N_{occ}/N_{orb}$ where N_{orb} is the number of orbitals per unit cell and N_{occ} is the filling, e.g. $\prod_{\mathbf{r}} \mathcal{O}_{\mathbf{R},\mathbf{r}}$ creates N_{occ} electrons. Eq. (1) ensures (2) holds, and we require that **(1)** and **(3)** are satisfied, as is natural in an insulator (see Supplementary Note 2).

We now define local RSIs in many-body atomic limits at a Wyckoff position $\mathbf{x}$ protected only by the symmetries of the point group $G_{\mathbf{x}} \in G$. To do so, we identify a set of discrete symmetry operators whose eigenvalues are the local RSIs. This ensures the local RSIs are adiabatic invariants since they are discrete quantum numbers. To ensure locality, we define the local RSI on OBCs by imposing a spatial cutoff around $\mathbf{x}$ and requiring invariance under the particular choice of cutoff.

Let $|GS, R\rangle$ be the groundstate of H_{AL} but restricted to OBCs by including only sites $|\mathbf{R}+\mathbf{r}-\mathbf{x}| \le R$ in Eq. (1) (see Fig. 1a). The cutoff breaks translational symmetry but preserves the point group symmetries $g \in G_{\mathbf{x}} \subset G$. The quantum numbers of $|GS, R\rangle$ are

$$\hat{N}|GS,R\rangle = N|GS,R\rangle, g|GS,R\rangle = e^{i\lambda[g]}|GS,R\rangle \tag{2}$$

where $\hat{N}$ is the number operator and $e^{i\lambda[g]}$ is a 1D irrep of $G_{\mathbf{x}}$. Note that $|GS,R\rangle$ is a non-degenerate trivial many-body atomic limit and must transform in a 1D irrep **(1)**. However, the quantum numbers N and $\lambda[g]$ are not independent of the cutoff, as we now show, so they cannot be local RSIs. Consider the spinless rotation groups $G_{\mathbf{x}} = n$ generated by the operator C_n. Because all terms in H_{AL} are strictly local **(2)**, we can write the groundstate at a larger cutoff $R' > R$ as

$$|GS,R'\rangle = \prod_{i=0}^{n-1} \mathcal{O}_i |GS,R\rangle, \quad \mathcal{O}_i = \prod_{\mathbf{R}+\mathbf{r}\in\mathcal{D}} C_n^i \mathcal{O}_{\mathbf{R},\mathbf{r}} C_n^{\dagger i} \tag{3}$$

where $\mathcal{D}$ is the annulus sector between R and R' of angle $2\pi/n$ shown in Fig. 1a and $C_n \in G_{\mathbf{x}}, C_n^n = +1$ is an n-fold rotation. Define the total charge $N_{\mathcal{O}}$ by $[\hat{N}, \mathcal{O}_i] = N_{\mathcal{O}}\mathcal{O}_i$ so that $\mathcal{O}_i\mathcal{O}_j = (-1)^{N_{\mathcal{O}}}\mathcal{O}_j\mathcal{O}_i$. Since the operators $\mathcal{O}_i$ commute/anti-commute if $N_{\mathcal{O}}$ is even/odd, Eq. (3) gives

$$C_n|GS,R'\rangle = e^{i\lambda[C_n]}(-1)^{N_{\mathcal{O}}}|GS,R'\rangle, \quad (n \text{ even}). \tag{4}$$

Thus the C_n eigenvalue $\lambda[C_n]$ is not invariant (for even n) under expanding the cutoff because $N_{\mathcal{O}}$ is arbitrary. Similarly, $\hat{N}|GS,R'\rangle = (N + nN_{\mathcal{O}})|GS,R'\rangle$ so N is clearly not invariant. However, we can easily produce symmetry operators which are invariant under an arbitrary expansion of the cutoff. Indeed, $e^{i\frac{\pi}{n}\hat{N}}C_n$ is invariant because

$$\begin{aligned} \langle GS,R'|e^{i\frac{\pi}{n}\hat{N}}C_n|GS,R'\rangle &= e^{i\frac{\pi}{n}(N+nN_{\mathcal{O}})}(-1)^{N_{\mathcal{O}}}e^{i\lambda[C_n]} \\ 1 em = e^{i\frac{\pi}{n}N}e^{i\lambda[C_n]} &= \langle GS,R|e^{i\frac{\pi}{n}\hat{N}}C_n|GS,R\rangle, \end{aligned} \tag{5}$$

and from Eq. (4), we see immediately that C_n^2 is also invariant (for n even). Hence we have found elementary symmetry operators whose eigenvalues only depend on the local properties of the groundstate near $\mathbf{x}$ but are invariant under the imposed cutoff. Their eigenvalues are the local RSIs defined by

$$\begin{aligned} e^{i\frac{\pi}{n}\hat{N}}C_n|GS\rangle &= e^{i\frac{\pi}{n}\Delta_1}|GS\rangle, \quad \Delta_1 \in \mathbb{Z}_{2n} \\ C_n^2|GS\rangle &= e^{i\frac{2\pi}{n/2}\Delta_2}|GS\rangle, \quad \Delta_2 \in \mathbb{Z}_{n/2} \end{aligned} \tag{6}$$

using $(e^{i\frac{\pi}{n}\hat{N}}C_n)^{2n} = (C_n^2)^{n/2} = +1$ which quantizes Δ_1, Δ_2. Although we derived Eq. (6) in many-body atomic limits, we now prove the local RSIs remain well-defined in general many-body atomic states. First, observe that the operators in Eq. (6) remain symmetries as hoppings and off-site interactions are added to H_{AL} and their eigenvalues (the local RSIs) remain well-defined. Then because we assume a many-body gap **(3)** and the local RSIs are quantized, they cannot change as H_{AL} is adiabatically deformed out of the strict atomic limit.

We have explicitly constructed local RSIs at a single Wyckoff position $\mathbf{x}$ on OBCs. But on infinite boundary conditions, the unit cell contains multiple Wyckoff positions and it should be possible to define local RSIs $\Delta_{\mathbf{x},1}, \Delta_{\mathbf{x},2}$ at each $\mathbf{x}$. For instance in the wallpaper group $G = p2$ which is generated by C_2 and translations, there are four Wyckoff positions 1a = (0, 0), 1b = (1/2, 0), 1c = (0, 1/2), and 1d = (1/2, 1/2) whose point groups are generated by C_2, T_1C_2, T_2C_2 and $T_1T_2C_2$ respectively. Even though imposing OBCs at one Wyckoff position breaks the symmetries of the others, we argue that the local RSIs are still well-

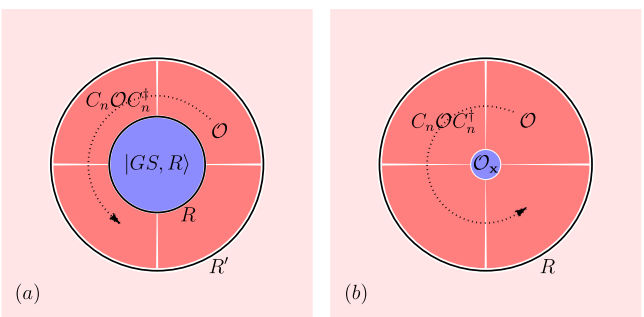

Fig. 1 | Local quantum numbers. a We depict the groundstate $|GS,R\rangle$ on OBCs and the additional symmetry-related operators which are included upon expanding the cutoff to R'. The many-body local RSIs are invariant under the expansion. **b** Given a fixed cutoff R, all operators inside of R but not at the C_n-invariant point $\mathbf{x}$ are symmetry-related and so do not contribute to the many-body local RSI. Only the operator $O_{\mathbf{x}}$ at $\mathbf{x}$ transforms locally under $\mathbf{x}$. Its quantum numbers determine the many-body local RSI.

defined on infinite boundary conditions. This is because the local RSIs are independent of the cutoff, so sending the cutoff to infinity recovers the full space group by restoring translations.

In Supplementary Note 2, we extend our results to construct local RSIs in all 2D spinless and spinful point groups (see Supplementary Tables 3 and 4). In the spinless groups, we find that mirrors and time-reversal restrict the C_n eigenvalue on the groundstate to be real, reducing the $\mathbb{Z}_{2n}\times\mathbb{Z}_{n/2}$ classification of Eq. (6) to $\mathbb{Z}_{2n}$ for even n. For odd n, we find a $\mathbb{Z}_n\times\mathbb{Z}_n$ classification which is reduced to $\mathbb{Z}_n$. For even n in the spinful groups, mirrors and time-reversal also force $C_n=\pm1$ to be real on any non-degenerate state, which yields a $\mathbb{Z}_2$ factor in the local RSI classification. We check that $C_n=+1$ holds on all product states (Slater determinants). The -1 eigenvalue is only possible with strong interactions, and can be obtained in trivial atomic Mott insulators[38,76]. In all cases, the classifying groups are abelian, so the local RSIs are additive: the local RSIs of a tensor product of states is the sum of their individual local RSIs. This is crucial for defining many-body fragile topology.

Many-body fragile topology

We now consider a state on infinite boundary conditions with charge density $\nu=N_{occ}/N_{orb}$. Recall that single-particle fragile topology is characterized by an obstruction to adiabatic deformation into an atomic state, but this obstruction is removed if additional (trivial) orbitals in a specific representation are added[6]. The topological indices for the single-particle fragile states are inequalities and mod equations relating N_{occ} and the RSIs in the unit cell[54].

This structure extends to the many-body case. We define a topological state with N_{occ} particles per unit cell as many-body fragile iff it can be adiabatically connected to a many-body trivial atomic state with $N_{occ}+\tilde{N}$ particles per unit cell by the addition of $\tilde{N}>0$ many-body atomic states[9,77]. Let $\Delta_{N_{occ}+\tilde{N}}$ (resp. $\Delta_{\tilde{N}}$) denote the set of RSIs of the trivial state with $N_{occ}+\tilde{N}$ particles (resp. the trivial state of the additional $\tilde{N}$ orbitals) at all Wyckoff positions in the unit cell. The local RSIs of the N_{occ}-particle many-body fragile state are defined by $\Delta_{frag}=\Delta_{N_{occ}+\tilde{N}}-\Delta_{\tilde{N}}$ (see Supplementary Note 3 for details). Crucially, $\Delta_{N_{occ}+\tilde{N}}$ is well-defined because the $N_{occ}+\tilde{N}$-particle state is trivial atomic. This underlies the essentially difference between fragile and stable topological many-body states (to be defined shortly), where the latter cannot be connected to any many-body atomic state via the addition of any many-body atomic states[54].

To assess whether a state is topological given a set of local RSIs, we can enumerate all possible atomic limits in G formed from N_{occ} orbitals — note that only a finite number are possible. If the local RSIs of the groundstate do not appear in this set, then the state must be fragile topological by definition. In practice, we find a simpler method by deriving inequality constraints that relate the local RSIs and the $U(1)$ electron density. To illustrate this, we again consider $G=p2$ with Wyckoff positions $\mathbf{x}=$1a,1b,1c,1d. There are four RSIs given by the eigenvalues $e^{i\frac{\pi}{2}\Delta_{1,\mathbf{x}}}$ of $e^{i\frac{\pi}{2}\hat{N}}C_{2,\mathbf{x}}$ where $C_{2,\mathbf{x}}$ is a rotation centered at $\mathbf{x}$. It is convenient to define $\Delta_{1,\mathbf{x}}\in\{-1,0,1,2\}$. For many-body atomic states on arbitrary OBCs respecting $G_{\mathbf{x}}$, it is easy to prove (see Supplementary Note 3) that $N_{\mathbf{x}}\geq|\Delta_{1,\mathbf{x}}|$ where $N_{\mathbf{x}}$ is the total number of particles. Note that $\Delta_{1\mathbf{x}}$ is does not depend on the OBC cutoff, whereas $N_{\mathbf{x}}$ obviously does. In a many-body atomic limit where we can take $N_{\mathbf{x}}=N_{\mathcal{O}}$ (see Eq. (3)) by choosing a cutoff surrounding $\mathbf{x}$ only (see Fig. 1b), we can bound the total density by summing over the number of states at the high-symmetry Wyckoff positions in a single unit cell:

$$N_{occ}\geq\sum_{\mathbf{x}=1a,1b,1c,1d}N_{\mathbf{x}}\geq\sum_{\mathbf{x}=1a,1b,1c,1d}|\Delta_{1,\mathbf{x}}| \tag{7}$$

which is a lower bound because only the high-symmetry Wyckoff positions are counted. The bound in Eq. (7) is ultimately written in terms of RSIs and the charge density which are well-defined quantum numbers in any many-body atomic state. Eq. (7) holds in all many-body atomic states. Hence if Eq. (7) is violated, then the RSIs impose an obstruction to deformation into a many-body atomic state, proving many-body fragile topology.

We can now prove that certain single-particle fragile states remain fragile topological as interactions are added. As a first step, we determine a formula for the local RSI when acting on product states (which are groundstates without interactions). With C_2, the irreps are A and B which are even and odd under C_2 respectively. Noting that $e^{i\frac{\pi}{2}\hat{N}}C_2|GS\rangle=e^{i\frac{\pi}{2}(m(A)+m(B))+i\pi m(B)}|GS\rangle$, Eq. (6) yields

$$\Delta_1=m(A)-m(B)\bmod 4 \tag{8}$$

where $m(\rho)$ is the multiplicity of the ρ irrep in the product state. In fact, this expression can be understood perturbatively. The single-particle RSI with C_2 is $\delta_1=m(B)-m(A)\in\mathbb{Z}$[54]. With interactions, a state with $m(A)=2$ can be scattered into a state with $m(B)=2$ since both have even parity. Thus states with $\delta_1=\pm2$ are identified with interactions[78], and only $\delta_1 \bmod 4=\Delta_1$ is invariant. Let us now consider the single-particle $N_{occ}=2$ fragile state $2\Gamma_1\oplus2X_1\oplus2Y_1\oplus2M_2=(A_{1a}\oplus A_{1b}\oplus A_{1c}\ominus A_{1d})\uparrow G$ which can be thought as stacking a Chern $+1$ state with a Chern -1 state. (Here $\uparrow$ denotes the Frobenius induction[47,54] of the irreps $\rho_{\mathbf{x}}\in G_{\mathbf{x}}$ to the full wallpaper group G containing all Wyckoff positions $\mathbf{x}$ as high symmetry points). Although their total Chern number vanishes, there is still fragile topology protected by C_2. We compute the RSIs to be $\Delta_{1a}=\Delta_{1b}=\Delta_{1c}=1$, $\Delta_{1d}=-1$. Evaluating the topological obstruction $\sum_{\mathbf{x}}|\Delta_{\mathbf{x}}|=4$ in Eq. (7), we find that this single-particle state violates the inequality since $N_{occ}=2$ and is many-body fragile. Adiabatically adding interactions cannot trivialize the state.

We generalize the inequality criterion of Eq. (7) to all wallpaper groups in Supplementary Note 3, obtaining topological invariants of many-body fragile phases. In Supplementary Table 5, we give expressions for the local RSIs on product states in terms of irrep multiplicities and also single-particle RSIs which are readily computed from momentum space irreps[54]. Our results determine the stability of any single-particle fragile phase when interactions are added.

Trivializing Single-Particle Fragile Topology

If the local RSIs are compatible with a many-body atomic state, our method indicates there is no obstruction to trivialization even if the single-particle RSIs are nontrivial. We now present an exactly solvable model where we adiabatically deform a single-particle fragile state into a single-particle trivial state through a strong coupling region[64].

Our strategy is to build a non-interacting Hamiltonian with fragile valence bands and obstructed atomic conduction bands. Importantly, we choose the conduction bands to have Wannier functions which are nonzero on a finite number of orbitals[79]. We choose $G=p3$ which has three Wyckoff positions shown in Fig. 2a. Each has spinless PG 3, whose irreps we denote A, ${}^1E$, ${}^2E$ carrying C_3 eigenvalues 1, $e^{i2\pi/3}$, $e^{-i2\pi/3}$ respectively. We create the atomic orbitals A_{1b}, ${}^2E_{1b}$, ${}^2E_{1c}$ and form the state

$$w^\dagger_{0,A_{1a}}|0\rangle=\tfrac{1}{3}\sum_{j=0}^{2}C_3^j(c^\dagger_{0,A_{1b}}+c^\dagger_{0,{}^2E_{1b}}+c^\dagger_{0,{}^2E_{1c}})|0\rangle \tag{9}$$

in the $\mathbf{R}=0$ unit cell and $w^\dagger_{\mathbf{R},A_{1a}}=T_{\mathbf{R}}w^\dagger_{0,A_{1a}}T^\dagger_{\mathbf{R}}$. $w^\dagger_{0,A_{1a}}$ creates an A irrep at 1a (see Fig. 2a). The complementary two bands on the A_{1b}, ${}^2E_{1b}$, ${}^2E_{1c}$ orbitals are fragile and cannot be induced from local orbitals (see Supplementary Note 5). We also add the atomic orbitals ${}^1E_{1a}$ and ${}^2E_{1a}$ to the valence band (which do not not trivialize the fragile topology) and a A_{1a} orbital to the conduction band. Note that A_{1a} would trivialize the valence band. To construct the non-interacting Hamiltonian H_0, we choose all bands to be perfectly flat so H_0 is local in the Wannier basis.

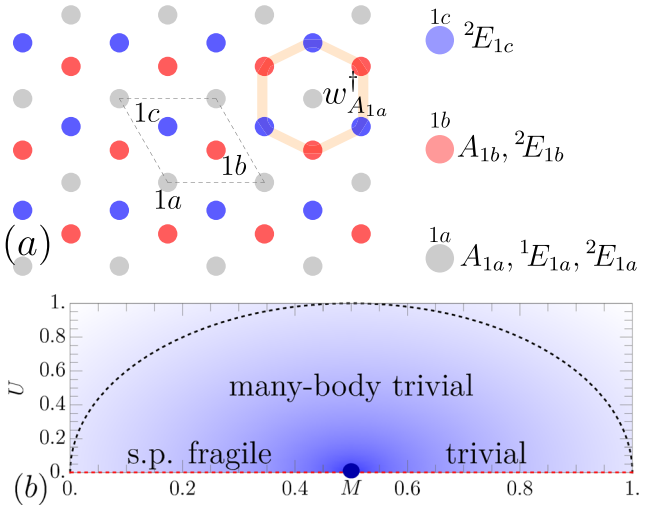

Fig. 2 | Trivializing fragile topology. a Orbitals and Wyckoff positions with $w^\dagger_{A_{1a}}$ shown in orange. **b** Phase diagram of $H_0 + H_I$ where shading denotes the many-body gap. The only gapless point (blue) occurs at $M = 1/2, U = 0$ separating the single-particle fragile and trivial phases at $U = 0$. Both phases have the same (trivial) many-body RSIs. Along the dashed line, the many-body gap is equal to 1 (see Supplementary Note 5).

As discussed in Supplementary Note 5, we set

$$H_0 = \sum_{\mathbf{R}} (1-M) w^\dagger_{\mathbf{R},A_{1a}} w_{\mathbf{R},A_{1a}} \\ 1em + M(n_{\mathbf{R},{}^1E_{1a}} + n_{\mathbf{R},{}^2E_{1a}}) + (1-M) n_{\mathbf{R},A_{1a}} \tag{10}$$

where $n_{\mathbf{R},\rho} = c^\dagger_{\mathbf{R},\rho} c_{\mathbf{R},\rho}$. All terms in H_0 are strictly local because $w_{\mathbf{R},A_{1a}}$ is finitely supported. At filling $\nu = N_{occ}/N_{orb} = 4/6$, M tunes between a fragile phase:

$$^1E_{1a} \oplus {}^2E_{1a} \oplus [A_{1b} \oplus {}^2E_{1b} \oplus {}^2E_{1c} \ominus A_{1a}] \uparrow G \tag{11}$$

for $M \in (0, 1/2)$ and a trivial phase $A_{1a} \oplus A_{1b} \oplus {}^2E_{1b} \oplus {}^2E_{1c}$ for $M \in (1/2, 1)$. The two fragile bands in Eq. (11) are in brackets. A gap closing at $M = 1/2$ separates the two phases. However Supplementary Table 5 shows the RSIs are the same in both phases: $\Delta_{1a} = (1, 0)$, $\Delta_{1b} = (2, 1)$, $\Delta_{1c} = (1, 1)$ and indicate a many-body atomic limit (as can be checked using the topological indices in Supplementary Table 8). Accordingly, the single-particle fragile phase can be connected to the trivial phase without a gap closing by adding interactions. We now add the symmetry-preserving term

$$H_I = U \sum_{\mathbf{R}} w^\dagger_{\mathbf{R},A_{1a}} c^\dagger_{\mathbf{R},A_{1a}} c_{\mathbf{R},{}^1E_{1a}} c_{\mathbf{R},{}^2E_{1a}} + h.c. \tag{12}$$

which is strictly local. Physically, H_I implements the interaction-allowed conversion[91] $E_{1a} \oplus {}^2E_{1a} \to A_{1a} \oplus A_{1a}$ and removes the fragile obstruction symbolized as $\ominus A_{1a}$ in Eq. (11) (but note that H_I annihilates the fragile bands). Because $H_0 + H_I$ acts independently on the Wannier states in each unit cell, the Hamiltonian is entirely decoupled and is trivial to solve[80]. We show the phase diagram in Fig. 2b and see that the gap closing at $U = 0$ separating the single-particle phases can be opened with interactions, adiabatically connecting the phases.

Many-body stable topology

Non-interacting stable topological states (such as Chern and quantum spin Hall insulators where many-body invariants are known[81–85]) cannot be trivialized by coupling to any local orbitals – unlike fragile topology. This is reflected in the single-particle RSIs, which take on fractional values in stable states[54]. For instance with C_2, the real-space derivation of the single-particle RSI $\delta_1 = m(A) - m(B) \in \mathbb{Z}$ relies on the existence of Wannier functions such that $m(A), m(B)$ are well-defined integers. It is only by generalizing the definition of δ_1 to momentum space (on periodic boundary conditions) that the possibility of fractional values emerges. In analogy to the non-interacting case, we define a many-body stable topological phase to be robust against coupling to all many-body atomic states. It is impossible to compute local (many-body) RSIs on OBCs in this case because the edge states, a signature of stable topology, prevent our assumption **(1)** of non-degeneracy and cannot be removed by coupling to any atomic states.

We now propose a definition of global RSIs $\Delta^G_{\mathbf{x},i}$ in many-body stable topological phases at Wyckoff position $\mathbf{x}$ in the unit cell. Their definition is identical to Eq. (6) but evaluated on a spatial torus, i.e. periodic boundary conditions (PBCs). Explicitly, with $C_n \in G_{\mathbf{x}}$ for n even,

$$e^{i\frac{\pi}{n}\hat{N}} C_n |GS, PBC\rangle = e^{i\frac{\pi}{n}\Delta^G_{\mathbf{x},1}} |GS, PBC\rangle, \\ C_n^2 |GS, PBC\rangle = e^{i\frac{2\pi}{n/2}\Delta^G_{\mathbf{x},2}} |GS, PBC\rangle \tag{13}$$

defines the global RSIs. The PBCs are essential for $|GS, PBC\rangle$ to be non-degenerate so $\Delta^G_{\mathbf{x},i}$ are quantum numbers. We claim that if $\Delta^G_{\mathbf{x},i} \neq 0, |GS, PBC\rangle$ is many-body stable topological. In other words, the global RSIs are topological invariants.

To support this claim, we prove two properties of $\Delta^G_{\mathbf{x},i}$: **(1)** All 2D many-body atomic phases have $\Delta^G_{\mathbf{x},i} = 0$, from which it follows that all many-body fragile topological phases also have $\Delta^G_{\mathbf{x},i} = 0$ and **(2)**: $\Delta^G_{\mathbf{x},i}$ is determined by the Chern number C in non-interacting Slater determinant states. This demonstrates the well-known fact that Chern insulators are robust to weak interactions.

We will first prove **(1)**. Consider a many-body atomic limit $\prod_{\mathbf{R},\mathbf{r}} \mathcal{O}_{\mathbf{R},|0\rangle}$ with $G = p2$ generated by $C_2, T_{\mathbf{R}}$ where $C_2 \in G_{\mathbf{x}}$ is a rotation around the point $\mathbf{x} = (0, 0)$. Now consider placing the state on $L_1 \times L_2$ PBCs with L_1, L_2 even. Observe that there are four points invariant under C_2 denoted $\mathbf{x}^G = \{(0, 0), (L_1/2, 0), (0, L_2/2), (L_1/2, L_2/2)\}$. Since the C_2 operator is a symmetry of each point, it protects a local RSI $\Delta_{\mathbf{x},1}$ given by $e^{i\frac{\pi}{2}\Delta_{1,\mathbf{x}}} \mathcal{O}_{\mathbf{x}} = (e^{i\frac{\pi}{2}\hat{N}} C_2) \mathcal{O}_{\mathbf{x}} (e^{i\frac{\pi}{2}\hat{N}} C_2)^\dagger$ for each $\mathbf{x} \in \mathbf{x}^G$. In fact, the $\Delta_{1,\mathbf{x}}$ is the same at each $\mathbf{x} \in \mathbf{x}^G$ because of translations: $\mathcal{O}_{\mathbf{x}} = T_{\mathbf{x}} \mathcal{O}_{(0,0)} T^\dagger_{\mathbf{x}}$ and $C_2 T_{\mathbf{x}} C_2^\dagger = T_{\mathbf{x}}$ since $\mathbf{x} = -\mathbf{x}$ for $\mathbf{x} \in \mathbf{x}^G$ on PBCs.

Now we compute the global RSI of the many-body atomic limit. Using the C_n symmetry, the atomic limit groundstate can generically be written as (see Fig. 3)

$$|GS, PBC\rangle = \prod_{\mathbf{x} \in \mathbf{x}^G} \mathcal{O}_{\mathbf{x}} \prod_{i=1}^{2} C_2^i \mathcal{O} C_2^{i\dagger} |0\rangle \tag{14}$$

for some $\mathcal{O}$ which creates the correlated but strictly local groundstates in one half of the spatial torus shown in Fig. 3. The operators $\mathcal{O}_{\mathbf{x}}$ create the states at the corners of the torus which are locally C_2 symmetric. Following Eq. (4), we compute

$$e^{i\frac{\pi}{2}\hat{N}} C_2 |GS, PBC\rangle = \prod_{\mathbf{x} \in \mathbf{x}^G} e^{i\frac{\pi}{2}\Delta_{\mathbf{x},1}} |GS, PBC\rangle \tag{15}$$

which is intuitive because operators $\mathcal{O}$ off the C_2 centers contribute trivially. Using Eq. (13), the global RSI of the many-body atomic state is

$$\Delta^G_{\mathbf{x},1} = \sum_{\mathbf{x} \in \mathbf{x}^G} \Delta_{\mathbf{x},1} = 4\Delta_{\mathbf{x},1} = 0 \bmod 4 \tag{16}$$

since we proved that $\Delta_{\mathbf{x},1}$ are all equal. The cancelation shown here is due to unexpected coincidence of the global RSI being defined mod 4, and the 4 C_2 symmetric points on PBCs each contributing an equal

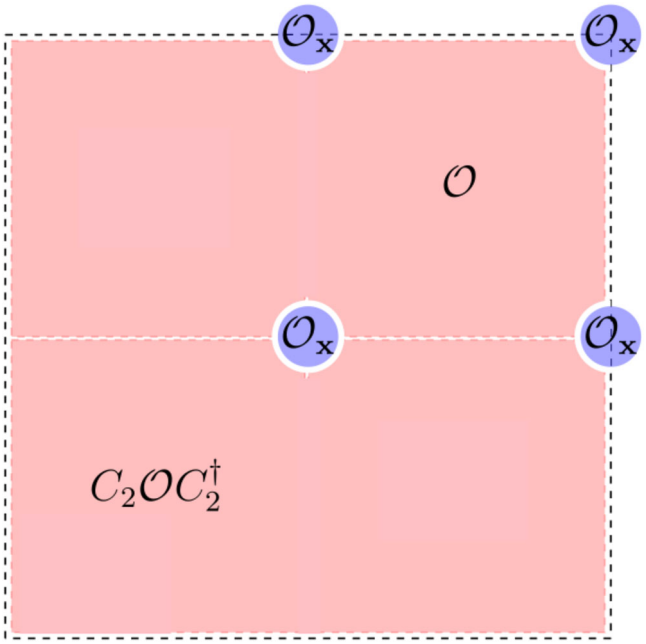

Fig. 3 | Local Operators on Periodic Boundary Conditions. We depict the partitioning of a many-body atomic limit state on a spatial torus (PBCs) into rotation-related operators $\mathcal{O}, C_2\mathcal{O}C_2^\dagger$ and the locally-transforming operators $\mathcal{O}_{\mathbf{x}}$ operators at fixed points of the rotation $\mathbf{x} \in \mathbf{x}^G$.

(integer) local RSI to the global RSIs. We extend this proof to all point groups in Supplementary Note 4.

Next to prove **(2)**, we relate $\Delta^G_{\mathbf{x},1}$ to the Chern number C in product states. We need two existing results. With C_2, $(-1)^C$ is equal to the product of inversion eigenvalues at the high-symmetry points in the Brillouin zone (BZ)[7,28,47,57,86], and secondly $C_2|GS, PBC\rangle = (-1)^C(-1)^{N/2}|GS, PBC\rangle$ where N is the number of states in the BZ which must be even since L_1, L_2 are even[87]. Evaluating the global RSI with Eq. (13) yields $\Delta^G_{1a,1} = 2C \bmod 4$. We can also compute $\Delta^G_{\mathbf{x},1}$ at other Wyckoff positions taking e.g. $C_2 \to T_1C_2$. Then because $|GS, PBC\rangle$ has zero total many-body momentum in 2D, we find

$$\Delta^G_{1a,1} = \Delta^G_{1b,1} = \Delta^G_{1c,1} = \Delta^G_{1d,1} = 2C \bmod 4. \tag{17}$$

This result is reminiscent of the half-integer valued single-particle RSIs in Chern insulators: Eq. (16) gives $\Delta^G_{\mathbf{x},1} = 4\Delta_{\mathbf{x},1}$ when local RSIs are well-defined, so Eq. (17) is suggestive of a half-integer local RSI in odd Chern states.

We compute the global RSIs of all Slater determinants in Supplementary Note 4. Our classification reveals the possibility of many stable topological phases which cannot exist in band theory but are enabled by strong interactions, agreeing with and extending earlier results[78,88,89]. We give a three illustrative examples. In $p2$, a state $|\psi\rangle$ with $\Delta^G_{1a,1} = \Delta^G_{1d,1} = 2, \Delta^G_{1b,1} = \Delta^G_{1c,1} = 0$ obeys $e^{i\frac{\pi}{2}\hat{N}}C_n|\psi\rangle = -|\psi\rangle$ like in a Chern state, but with nonzero total momentum $T_1|\psi\rangle = T_2|\psi\rangle = -|\psi\rangle$. Such a state carries a many-body Chern number[28], but is adiabatically disconnected from any single-particle Chern state. In $p2mm$, mirrors ensure $C = -C = 0$ without interactions. But the global RSI Δ^G_1 retains a $\mathbb{Z}_4$ classification after adding mirrors, allowing an interaction-enabled state like Eq. (17) following the heuristic $2C = -2C \bmod 4$[90]. Finally, Eq. (17) shows that $\Delta^G_{\mathbf{x},1}$ must be even in gapped Slater determinants. Since an $\Delta^G_{\mathbf{x},1}$ odd requires odd particle number but L_1, L_2 are even, this suggests a gapless state. This is evidence that odd $\Delta^G_{\mathbf{x},1}$, defined by Eq. (13), is a many-body semi-metal invariant[91,92].

Topological response theory

RSIs are quantized, symmetry-protected invariants beyond the Chern number. Then, since a nonzero Chern number is encoded in the continuum topological response theory as a Chern-Simons term[93], it might be expected that RSIs appear as well. In the presence of crystalline symmetries, the response theory includes Wen-Zee-type terms[14,19,31,94–102]:

$$\mathcal{L} = \frac{C}{4\pi} A\, dA + \frac{s}{2\pi} A\, d\omega + \frac{\ell}{4\pi} \omega\, d\omega \tag{18}$$

where $A = A_\mu dx^\mu$ is the $U(1)$ gauge field and $\omega = \omega_\mu dx^\mu$ is the rotational gauge field, or spin connection[10,31,97,103]. Physically, $\int dA$ and $\int d\omega$ are the total flux and total disclination angle. Eq. (18) neglects translational gauge fields[95,104] and hence ignores the unit cell structure, so $\mathcal{L}$ describes an expansion around a fixed Wyckoff position $\mathbf{x}$. We will show that s and ℓ are the local RSIs at $\mathbf{x}$.

The coefficients s and ℓ can be understood from the equation of motion for the charge density ρ and angular momentum density L:

$$\rho = \frac{\delta \mathcal{L}}{\delta A_0} = \frac{C}{2\pi} dA + \frac{s}{2\pi} d\omega, L = \frac{\delta \mathcal{L}}{\delta \omega_0} = \frac{s}{2\pi} dA + \frac{\ell}{2\pi} d\omega. \tag{19}$$

Let us first consider ρ. If $d\omega = 0$, Eq. (19) reduces to the Streda formula[105]. If $dA = 0, s$ describes the charge bound to a disclination center. A partial disclination with $s \neq 0$ reveals the fractional charge at $\mathbf{x}$[33,98,106,107]. As such, taking $\int d\omega = 2\pi$ to be a complete disclination (in analogy to inserting a full flux), Eq. (19) shows $s = \int \rho$ is the total charge at $\mathbf{x}$. Since the total charge is related to the local RSIs, Eq. (6) gives (for n even)

$$e^{i\frac{2\pi}{n}s} = e^{i\frac{2\pi}{n}\hat{N}} = (e^{i\frac{\pi}{n}\hat{N}}C_n)^2 (C_n^2)^\dagger = e^{i\frac{2\pi}{n}(\Delta_{1,\mathbf{x}} - 2\Delta_{2,\mathbf{x}})} \tag{20}$$

acting on $|GS\rangle$ with OBCs. Hence s is the local charge

$$s = \Delta_{1,\mathbf{x}} - 2\Delta_{2,\mathbf{x}} \bmod n \quad (n \text{ even}). \tag{21}$$

We remark that the physical charge bound to the disclination core is a well-defined local observable and can take any (rational) value. However, Eq. (21) shows that its value mod n is determined solely by the many-body RSIs of the defect-less groundstate and is universal. This can be understood from the Lagrangian in Eq. (18): although $\mathcal{L}$ is well-defined for all s, adiabatic deformations of the groundstate leave only s mod n constant. In many-body fragile or atomic states where $\Delta_{i,\mathbf{x}}$ are integers, $s \in \mathbb{Z}_n$. Eq. (21) suggests a straightforward generalization to Chern states. Without interactions, the single-particle local RSIs are well-defined but fractional, and a formula for the charge s at $\mathbf{x}$ is known[54,59]. Proving the many-body extension of this result will be the subject of forthcoming work. For now in the C_2 case, note that Eq. (16) (proved only at $C = 0$) shows $4\Delta_{\mathbf{x},1} = \Delta^G_{\mathbf{x},1}$, while Eq. (17) shows $\Delta^G_{\mathbf{x},1} = 2C \bmod 4$. Then at least heuristically, the local RSI $\Delta_{\mathbf{x},1} = C/2 \bmod 4$ can be half-integer in agreement with ref. 98.

We now consider L in Eq. (19). Setting $d\omega = 0$ shows that s shifts the angular momentum after inserting a full flux. Indeed, single-particle RSIs can enforce irrep flow due to angular momentum pumping in flux[59,108]. Setting $dA = 0$ shows that ℓ describes the angular momentum bound to a disclination center and should be identified with the eigenvalue of the rotation operator $e^{i\frac{\pi}{n}\hat{N}}C_n$. Hence we propose $\ell = \Delta_{1,\mathbf{x}} \in \mathbb{Z}_{2n}$ for n even, matching the classification of ref. 98.

Discussion

TQC is a unifying theory of non-interacting materials. Given atomic orbitals, their symmetries, and the number of electrons, the topological invariants of TQC classify possible gapped, degenerate, and gapless phases. The present work achieves the first case in interacting

Hamiltonians by defining local and global RSIs, many-body topological indices, and the effective field theory that governs them. In so doing, we revealed which single-particle fragile phases survive interactions and identified undiscovered stable topological states with no single-particle counterpart. We anticipate that many features of single-particle topology may be generalized to the many-body case using this formalism, for instance regarding bounds on quantum geometry[15,109–114]. Another perspective is offered by ref. 28, which shows that a generalization of the single-particle Brillouin zone is the flux torus obtained from twisted boundary conditions (on which the gapped, many-body groundstate can smoothly be defined), since in both cases the Berry curvature and symmetry eigenvalues can be defined. This connection may facilitate the computation of many-body RSIs without open boundary conditions and reveal connections between the momentum space and real space theories. We leave the study of global and magnetic symmetries, spontaneous symmetry breaking, the numerical investigation of interaction-enabled many-body stable topology, and the study of boundary signatures to future work.

Inclusion and ethics

A portion of this work was completed at Princeton University, which occupies part of the ancient homeland and traditional territory of the Lenape people. We pay respect to Lenape peoples past, present, and future and their continuing presence in the homeland and throughout the Lenape diaspora.

Data availability

All data the supporting the findings of this study are available form the authors upon reasonable request.

References

1. Ryu, S., Schnyder, A. P., Furusaki, A. & Ludwig, AndreasW. W. Topological insulators and superconductors: tenfold way and dimensional hierarchy. *N. J. Phys.* **12**, 065010 (2010).
2. Kitaev, A. Periodic table for topological insulators and superconductors. In Vladimir Lebedev and Mikhail Feigel'Man, editors, *American Institute of Physics Conference Series*, volume 1134 of *American Institute of Physics Conference Series*, pages 22–30, May (2009). https://doi.org/10.1063/1.3149495.
3. Bradlyn, B. et al. Topological quantum chemistry. *Nat. (Lond.)* **547**, 298–305 (2017).
4. Elcoro, L. et al. Magnetic topological quantum chemistry. *Nat. Commun.* **12**, 5965 (2021).
5. Aroyo, M. I., Kirov, A., Capillas, C., Perez-Mato, J. M. & Wondratschek, H. Bilbao Crystallographic Server. II. Representations of crystallographic point groups and space groups. *Acta Crystallogr. Sect. A* **62**, 115–128 (2006).
6. Song, Z.-D., Elcoro, L., Xu, Y.-F. Regnault, N. & Bernevig, B. A. Fragile phases as affine monoids: classification and material examples. *Physical Review X* **10**, 031001 (2020).
7. Po, H., Vishwanath, A. & Watanabe, H. Complete theory of symmetry-based indicators of band topology. *Nat. Commun.* **8**, 50 (2017).
8. Kruthoff, J., de Boer, J., van Wezel, J., Kane, C. L. & Slager, Robert-Jan Topological classification of crystalline insulators through band structure combinatorics. *Phys. Rev. X* **7**, 041069 (2017).
9. Else, D. V., Po, HoiChun & Watanabe, H. Fragile topological phases in interacting systems. *Phys. Rev. B* **99**, 125122 (2019).
10. Thorngren, R. & Else, D. V. Gauging spatial symmetries and the classification of topological crystalline phases. *Phys. Rev. X* **8**, 011040 (2018).
11. Lessnich, D., Winter, S. M., Iraola, M., Vergniory, M. G. & Valentí, R. Elementary band representations for the single-particle Green's function of interacting topological insulators. *Phys. Rev. B* **104**, 085116 (2021).
12. Iraola, M. et al. Towards a topological quantum chemistry description of correlated systems: The case of the Hubbard diamond chain. *Phys. Rev. B Nature Physics* **104**, 195125 (2021).
13. Misawa, T. & Yamaji, Y. Zeros of Green functions in topological insulators. *Phys. Rev. Res.* **4**, 023177 (2022).
14. Barkeshli, M., Chen, Y.-A., Hsin, P.-S. & Manjunath, N. Classification of (2+1)D invertible fermionic topological phases with symmetry. *Phys. Rev. B* **105**, 235143 (2022).
15. Herzog-Arbeitman, J., Peri, V., Schindler, F., Huber, S. D. & Bernevig, B. A. Superfluid weight bounds from symmetry and quantum geometry in flat bands. *Phys. Rev. Lett.* **128**, 087002 (2022).
16. Chen, L. et al. Topological semimetal driven by strong correlations and crystalline symmetry. *Nat. Phys.* **18**, 1341–1346 (2022).
17. Isobe, H. & Fu, L. Theory of interacting topological crystalline insulators. *Phys. Rev. B* **92**, 081304 (2015).
18. Herzog-Arbeitman, J., Chew, A., Huhtinen, Kukka-Emilia, Törmä, Päivi, and Bernevig, B. A. Many-Body superconductivity in topological flat bands. Preprint at *arXiv e-prints*, art. arXiv:2209.00007, August (2022).
19. Huang, S.-J., Hsieh, Chang-Tse & Yu, J. Effective field theories of topological crystalline insulators and topological crystals. *Phys. Rev. B* **105**, 045112 (2022).
20. Lu, Yuan-Ming & Vishwanath, A. Theory and classification of interacting integer topological phases in two dimensions: A chern-simons approach. *Phys. Rev. B* **86**, 125119 (2012).
21. Peotta, S. & Törmä, P. äivi Superfluidity in topologically nontrivial flat bands. *Nat. Commun.* **6**, 8944 (2015).
22. Bernevig, B. A. et al. Twisted bilayer graphene. v. exact analytic many-body excitations in coulomb hamiltonians: Charge gap, goldstone modes, and absence of cooper pairing. *Phys. Rev. B* **103**, 205415 (2021).
23. Herzog-Arbeitman, J., Chew, A., Efetov, D. K. & Bernevig, B. A. Reentrant correlated insulators in twisted bilayer graphene at 25 T (2 π Flux). *Phys. Rev. Lett.* **129**, 076401 (2022).
24. Xie, F., Song, Z., Lian, B. & Bernevig, B. A. Topology-bounded superfluid weight in twisted bilayer graphene. *Phys. Rev. Lett.* **124**, 167002 (2020).
25. Chiu, C.-K., Teo, Jeffrey, C. Y., Schnyder, A. P. & Ryu, S. Classification of topological quantum matter with symmetries. *Rev. Mod. Phys.* **88**, 035005 (2016).
26. Han, B., Tiwari, A., Hsieh, Chang-Tse & Ryu, S. Boundary conformal field theory and symmetry-protected topological phases in 2 +1 dimensions. *Phys. Rev. B* **96**, 125105 (2017).
27. Klein Kvorning, T., Spânslätt, C., Chan, At. MaP. O. & Ryu, S. Nonlocal order parameters for states with topological electromagnetic response. *Phys. Rev. B* **101**, 205101 (2020).
28. Matsugatani, A., Ishiguro, Y., Shiozaki, K. & Watanabe, H. Universal relation among the many-body chern number, rotation symmetry, and filling. *Phys. Rev. Lett.* **120**, 096601 (2018).
29. Shiozaki, K., Shapourian, H., Gomi, K. & Ryu, S. Many-body topological invariants for fermionic short-range entangled topological phases protected by antiunitary symmetries. *Phys. Rev. B* **98**, 035151 (2018).
30. Wang, J., Cano, J., Millis, A. J., Liu, Z. & Yang, B. Exact landau level description of geometry and interaction in a flatband. *Phys. Rev. Lett.* **127**, 246403 (2021).
31. Manjunath, N. & Barkeshli, M. Crystalline gauge fields and quantized discrete geometric response for Abelian topological phases with lattice symmetry. *Phys. Rev. Res.* **3**, 013040 (2021).
32. Wang, Q.-R., Qi, Y., Fang, C., Cheng, M. & Gu, Z.-C. Exactly solvable lattice models for interacting electronic insulators in two dimensions. *Phys. Rev. B* **108**, L121104 (2023).

33. May-Mann, J. & Hughes, T. L. Crystalline responses for rotation-invariant higher-order topological insulators. *Phys. Rev. B* **106**, L241113 (2022).
34. Sen, S., Wong, P. J. & Mitchell, A. K. The Mott transition as a topological phase transition. *Phys. Rev. B* **102**, 081110 (2020).
35. Fan, R., Sahay, R. & Vishwanath, A. Extracting the Quantum Hall Conductance from a Single Bulk Wave Function. *Phys. Rev. Lett.* **131**, 186301 (2023).
36. Rachel, S. Interacting topological insulators: a review. *Rep. Prog. Phys.* **81**, 116501 (2018).
37. Kashihara, T., Michishita, Y. & Peters, R. Quantum metric on the brillouin zone in correlated electron systems and its relation to topology for chern insulators. *Phys. Rev. B* **107**, 125116 (2023).
38. Soldini, M. O. et al. Interacting topological quantum chemistry of Mott atomic limits. *Phys. Rev. B* **107**, 245145 (2023).
39. Bouhon, A., Black-Schaffer, A. M. & Slager, R.-J. Wilson loop approach to fragile topology of split elementary band representations and topological crystalline insulators with time-reversal symmetry. *Phys. Rev. B* **100**, 195135 (2019).
40. Ahn, J., Park, S. & Yang, B.-J. Failure of nielsen-ninomiya theorem and fragile topology in two-dimensional systems with space-time inversion symmetry: application to twisted bilayer graphene at magic angle. *Phys. Rev. X* **9**, 021013 (2019).
41. Song, Z.-D. et al. All magic angles in twisted bilayer graphene are topological. *Phys. Rev. Lett.* **123**, 036401 (2019).
42. Alexandradinata, A., Dai, X. & Bernevig, B. A. Wilson-loop characterization of inversion-symmetric topological insulators. *Phys. Rev.* **B89**, 155114 (2014).
43. Yu, R., Qi, X., Bernevig, A., Fang, Z. & Dai, X. Equivalent expression of Z_2 topological invariant for band insulators using the non-Abelian Berry connection. *Phys. Rev. B* **84**, 075119 (2011).
44. Yang, S.-Y. et al. Symmetry demanded topological nodal-line materials. *Adv. Phys. X* **3**, 1414631 (2018).
45. Benalcazar, W. A., Bernevig, B. A. & Hughes, T. L. Quantized electric multipole insulators. *Science* **357**, 61–66 (2017).
46. Bernevig, B. A. & Hughes, T. L. Topological Insulators and Topological Superconductors. Princeton University Press, student edn., ISBN 9780691151755. http://www.jstor.org/stable/j.ctt19cc2gc (2013).
47. Cano, J. & Bradlyn, B. B. Band Representations and Topological Quantum Chemistry. *Annu. Rev. Condens. Matter Phys.* **12**, 225–246 (2021).
48. Watanabe, H., Po, H. & Vishwanath, A. Structure and topology of band structures in the 1651 magnetic space groups. *Sci. Adv.* **4**, eaat8685 (2018).
49. Khalaf, E., Po, H., Vishwanath, A. & Watanabe, H. Symmetry indicators and anomalous surface states of topological crystalline insulators. *Phys. Rev. X* **8**, 031070 (2018).
50. Song, Z., Zhang, T., Fang, Z. & Fang, C. Quantitative mappings between symmetry and topology in solids. *Nat. Commun.* **9**, 3530 (2018).
51. Marzari, N., Mostofi, A. A., Yates, J. R., Souza, I. & Vanderbilt, D. Maximally localized Wannier functions: theory and applications. *Rev. Mod. Phys.* **84**, 1419–1475 (2012).
52. Soluyanov, A. A. & Vanderbilt, D. Wannier representation of Z_2 topological insulators. *Phys. Rev. B* **83**, 035108 (2011).
53. Brouder, C., Panati, G., Calandra, M., Mourougane, C. & Marzari, N. Exponential localization of wannier functions in insulators. *Phys. Rev. Lett.* **98**, 046402 (2007).
54. Song, Z.-D., Elcoro, L. & Bernevig, B. A. Twisted bulk-boundary correspondence of fragile topology. *Science* **367**, 794–797 (2020).
55. Po, H., Watanabe, H. & Vishwanath, A. Fragile topology and wannier obstructions. *Phys. Rev. Lett.* **121**, 126402 (2018).
56. Cano, J. et al. Topology of disconnected elementary band representations. *Phys. Rev. Lett.* **120**, 266401 (2018).
57. Po, H. Symmetry indicators of band topology. *J. Phys. Condens. Matter* **32**, 263001 (2020).
58. Xu, Y. et al. Three-dimensional real space invariants, obstructed atomic insulators and a new principle for active catalytic sites. Preprint at *arXiv e-prints*, art. arXiv:2111.02433, November (2021).
59. Herzog-Arbeitman, J., Song, Z.-D., Elcoro, L. & Bernevig, B. A. Hofstadter Topology with Real Space Invariants and Reentrant Projective Symmetries. *Phys. Rev. Lett.***130**, 236601 (2023).
60. Gurarie, V. Single-particle Green's functions and interacting topological insulators. *Phys. Rev. B* **83**, 085426 (2011).
61. Essin, A. M. & Gurarie, V. Bulk-boundary correspondence of topological insulators from their respective Green's functions. *Phys. Rev. B* **84**, 125132 (2011).
62. Zhang, J.-H., Yang, S., Qi, Y. & Gu, Z.-C. Real-space construction of crystalline topological superconductors and insulators in 2d interacting fermionic systems. *Phys. Rev. Res.* **4**, 033081 (2022).
63. Tran, M.-T., Nguyen, D.-B., Nguyen, H.-S. & Tran, T.-M. Topological green function of interacting systems. *Phys. Rev. B* **105**, 155112 (2022).
64. Fidkowski, L. & Kitaev, A. Effects of interactions on the topological classification of free fermion systems. *Phys. Rev. B* **81**, 134509 (2010).
65. Song, Z., Fang, Z. & Fang, C. (d -2) -Dimensional edge states of rotation symmetry protected topological states. *Phys. Rev. Lett.* **119**, 246402 (2017).
66. Schindler, F., Bradlyn, B., Fischer, M. H. & Neupert, T. Pairing obstructions in topological superconductors. *Phys. Rev. Lett.* **124**, 247001 (2020).
67. Benalcazar, W. A. et al. Higher-order topological pumping and its observation in photonic lattices. *Phys. Rev. B* **105**, 195129 (2022).
68. Benalcazar, W. A., Bernevig, B. A. & Hughes, T. L. Electric multipole moments, topological multipole moment pumping, and chiral hinge states in crystalline insulators. *Phys. Rev. B* **96**, 245115 (2017).
69. Po, H.C., Zou, L., Senthil, T. & Vishwanath, A. Faithful Tight-binding Models and Fragile Topology of Magic-angle Bilayer Graphene. *Phys. Rev. B*, **99**, 195455 (2019).
70. Peri, V., Song, Z.-D., Bernevig, B. A. & Huber, S. D. Fragile topology and flat-band superconductivity in the strong-coupling regime. *Phys. Rev. Lett.* **126**, 027002 (2021).
71. Peri, V. et al. Experimental characterization of fragile topology in an acoustic metamaterial. *Science* **367**, 797–800 (2020).
72. Wieder, B. J. & Bernevig, B. A. The Axion Insulator as a Pump of Fragile Topology. Preprint at *arXiv e-prints*, art. arXiv:1810.02373, Oct (2018).
73. Haldane, F. D. M. Model for a quantum hall effect without landau levels: condensed-matter realization of the "parity anomaly". *Phys. Rev. Lett.* **61**, 2015–2018 (1988).
74. Bernevig, B. A., Hughes, T. L. & Zhang, Shou-Cheng Quantum spin hall effect and topological phase transition in hgte quantum wells. *Science* **314**, 1757 (2006).
75. Kane, C. L. & Mele, E. J. Z_2 Topological order and the quantum spin hall effect. *Phys. Rev. Lett.* **95**, 146802 (2005).
76. Yao, H. & Kivelson, S. A. Fragile mott insulators. *Phys. Rev. Lett.* **105**, 166402 (2010).
77. Latimer, K. & Wang, C. Correlated fragile topology: A parton approach. *Phys. Rev. B* **103**, 045128 (2021).
78. Liu, S., Vishwanath, A. & Khalaf, E. Shift insulators: rotation-protected two-dimensional topological crystalline insulators. *Phys. Rev. X* **9**, 031003 (2019).
79. Schindler, F. & Bernevig, B. A. Noncompact atomic insulators. *Phys. Rev. B* **104**, L201114 (2021).

80. Mizoguchi, T., Kuno, Y. & Hatsugai, Y. Construction of interacting flat-band models by molecular-orbital representation: Correlation functions, energy gap, and entanglement. *Prog. Theor. Exp. Phys.* **2022**, 023I02 (2022).
81. Thouless, D. J., Kohmoto, M., Nightingale, M. P. & den Nijs, M. Quantized hall conductance in a two-dimensional periodic potential. *Phys. Rev. Lett.* **49**, 405–408 (1982).
82. Fu, L. & Kane, C. L. Time reversal polarization and a Z_2 adiabatic spin pump. *Phys. Rev. B* **74**, 195312 (2006).
83. Dehghani, H., Cian, Z.-P., Hafezi, M. & Barkeshli, M. Extraction of the many-body Chern number from a single wave function. *Phys. Rev. B* **103**, 075102 (2021).
84. Wang, Z. & Zhang, S.-C. Simplified topological invariants for interacting insulators. *Phys. Rev. X* **2**, 031008 (2012).
85. Lee, S.-S. & Ryu, S. Many-body generalization of the Z_2 topological invariant for the quantum spin hall effect. *Phys. Rev. Lett.* **100**, 186807 (2008).
86. Hughes, T. L., Prodan, E. & Bernevig, B. A. Inversion-symmetric topological insulators. *Phys. Rev. B* **83**, 245132 (2011).
87. Fang, C., Gilbert, M. J. & Bernevig, B. A. Entanglement spectrum classification of C_n-invariant noninteracting topological insulators in two dimensions. *Phys. Rev. B* **87**, 035119 (2013).
88. Shapourian, H., Shiozaki, K. & Ryu, S. Many-body topological invariants for fermionic symmetry-protected topological phases. *Phys. Rev. Lett.* **118**, 216402 (2017).
89. Shiozaki, K., Shapourian, H. & Ryu, S. Many-body topological invariants in fermionic symmetry-protected topological phases: Cases of point group symmetries. *Phys. Rev. B* **95**, 205139 (2017).
90. Lapa, M. F., Teo, J. C. Y. & Hughes, T. L. Interaction-enabled topological crystalline phases. *Phys. Rev. B* **93**, 115131 (2016).
91. Song, Z., Zhang, T. & Fang, C. Diagnosis for nonmagnetic topological semimetals in the absence of spin-orbital coupling. *Phys. Rev. X* **8**, 031069 (2018).
92. Huang, S.-J., Yu, J. & Zhang, R.-X. Classification of interacting dirac semimetals. Preprint at *arXiv e-prints*, art. arXiv:2211.03802, November (2022).
93. Qi, X.-L., Hughes, T. L. & Zhang, S.-C. Topological field theory of time-reversal invariant insulators. *Phys. Rev. B* **78**, 195424 (2008).
94. Wen, X. G. & Zee, A. Shift and spin vector: New topological quantum numbers for the hall fluids. *Phys. Rev. Lett.* **69**, 953–956 (1992).
95. Hung, L.-Y. & Wen, X.-G. Quantized topological terms in weak-coupling gauge theories with a global symmetry and their connection to symmetry-enriched topological phases. *Phys. Rev. B* **87**, 165107 (2013).
96. Wen, X.-G. Classifying gauge anomalies through symmetry-protected trivial orders and classifying gravitational anomalies through topological orders. *Phys. Rev. D.* **88**, 045013 (2013).
97. Abanov, A. G. & Gromov, A. Electromagnetic and gravitational responses of two-dimensional noninteracting electrons in a background magnetic field. *Phys. Rev. B* **90**, 014435 (2014).
98. Zhang, Y., Manjunath, N., Nambiar, G. & Barkeshli, M. Fractional disclination charge and discrete shift in the Hofstadter butterfly. *Phys. Rev. Lett.* **129**, 275301 (2022).
99. Mera, B. Topological response of gapped fermions to a $\mathrm{U}(1)$ Gauge field. Preprint at *arXiv e-prints* **129**, 1705.04394 (2017).
100. Bradlyn, B. & Read, N. Topological central charge from berry curvature: gravitational anomalies in trial wave functions for topological phases. *Phys. Rev. B* **91**, 165306 (2015).
101. Bradlyn, B. & Read, N. Low-energy effective theory in the bulk for transport in a topological phase. *Phys. Rev. B* **91**, 125303 (2015).
102. Rao, P. and Bradlyn, B. Effective action approach to the filling anomaly in crystalline topological matter, URL https://arxiv.org/abs/2302.11602 (2023).
103. Else, D. V., Huang, Sheng-Jie, Prem, A. & Gromov, A. Quantum many-body topology of quasicrystals. *Phys. Rev. X* **11**, 041051 (2021).
104. Zhang, Y., Manjunath, N., Nambiar, G. & Barkeshli, M. Quantized charge polarization as a many-body invariant in (2+1)D crystalline topological states and Hofstadter butterflies. *Phys. Rev. X.* **13**, 031005 (2023).
105. Streda, P. Theory of quantised Hall conductivity in two dimensions. *J. Phys. C. Solid State Phys.* **15**, L717–L721 (1982).
106. Li, T., Zhu, P., Benalcazar, W. A. & Hughes, T. L. Fractional disclination charge in two-dimensional C_n-symmetric topological crystalline insulators. *Phys. Rev. B* **101**, 115115 (2020).
107. Jiang, G., Chen, Y., Iyer-Biswas, S. & Biswas, R. R. Gravitational response of topological quantum states of matter. *Phys. Rev. B* **107**, 195403 (2023).
108. Herzog-Arbeitman, J., Song, Zhi-Da, Regnault, N. & Bernevig, B. A. Hofstadter topology: noncrystalline topological materials at high flux. *Phys. Rev. Lett.* **125**, 236804 (2020).
109. Kashihara, T., Michishita, Y. & Peters, R. Quantum metric on the Brillouin zone in correlated electron systems and its relation to topology for Chern insulators. *Phys. Rev. B* **107**, 125116 (2023).
110. Salerno, G., Ozawa, T. & Törmä, P. Drude weight and the many-body quantum metric in one-dimensional bose systems. *Phys. Rev. B* **108**, L140503 (2023).
111. Verma, N., Hazra, T. & Randeria, M. Optical spectral weight, phase stiffness, and T_c bounds for trivial and topological flat band superconductors. *Proc. Natl Acad. Sci. USA* **118**, e2106744118 (2021).
112. Mao, D. & Chowdhury, D. Diamagnetic response and phase stiffness for interacting isolated narrow bands. *Proc. Natl Acad. Sci. USA* **120**, e2217816120 (2023).
113. Aroyo, M. I. et al. Bilbao crystallographic server: I. databases and crystallographic computing programs. *ZEITSCHRIFT FUR KRISTALLOGRAPHIE* **221**, 15–27 (2006).
114. Fang, C., Gilbert, M. J. & Bernevig, B. A. Bulk topological invariants in noninteracting point group symmetric insulators. *Phys. Rev. B* **86**, 115112 (2012).

Acknowledgements

We thank Adrian Po for influential comments in the early stages of this work and Abhinav Prem for his insight and careful explanations. Additionally we thank Frank Schindler for useful guidance, Jiabin Yu, and Biao Lian for enlightening consultations, and Titus Neupert, Glenn Wagner, and Martina Soldini for sharing their unpublished paper on many-body atomic limits in the final states of this work. JHA thanks the Donostia International Physics Center for their hospitality during the completion of this manuscript. B.A.B. and Z-D.S. were supported by the European Research Council (ERC) under the European Union's Horizon 2020 research and innovation programme (grant agreement No. 101020833), the ONR Grant No. N00014-20-1-2303, the Schmidt Fund for Innovative Research, Simons Investigator Grant No. 404513, the Packard Foundation, the Gordon and Betty Moore Foundation through the EPiQS Initiative, Grant GBMF11070 and Grant No. GBMF8685 towards the Princeton theory program. Further support was provided by the NSF-MRSEC Grant No. DMR-2011750, BSF Israel US foundation Grant No. 2018226, and the Princeton Global Network Funds. JHA is supported by a Hertz Fellowship and ONR Grant No. N00014-20-1-2303, as well as a Marshall Scholarship during the early stages of this project.

Author contributions

JHA, BAB, and ZDS all contributed to the intellectual content of the work.

Competing interests

The authors declare no competing interests.

Additional information

Supplementary information The online version contains supplementary material available at https://doi.org/10.1038/s41467-024-45395-9.

Correspondence and requests for materials should be addressed to Jonah Herzog-Arbeitman.

Peer review information *Nature Communications* thanks the anonymous reviewers for their contribution to the peer review of this work. A peer review file is available.